



Polar cap convection events and electrojet intensifications during Earth passage of interplanetary CME's

Y. L. Andalsvik¹, P. E. Sandholt¹, C. J. Farrugia²

¹ Department of Physics, University of Oslo, Norway. ²Space Science Center, University of New Hampshire, Durham, NH, USA



Introduction

■ We investigate the association between temporal/spatial structure of polar cap convection and auroral electrojet intensifications during intervals of strong forcing of the magnetosphere in association with Earth passage of interplanetary CMEs (ACE/Wind data).

■ The main data base: Coordinated ground - satellite observations in the 1500-2000 MLT sector.

■ We take advantage of the good latitudinal coverage in the polar cap and in the auroral zone of the IMAGE chain of ground magnetometers in Svalbard - Scandinavia - Russia and the stable magnetic field conditions in ICMEs.

■ The events are characterized by a series of 10 min-long AL - excursions to -1000/-1500 nT superimposed on a high disturbance level when the AL index \sim -500 nT for several hours. These signatures are very different from those appearing in classical substorms, most notably the absence of a complete recovery phase when AL usually reaches above -100 nT.

■ We study temporal and spatial structure in polar cap convection in both hemispheres (DMSP F13 data) in relation to IMF conditions, electrojet intensifications, and poleward boundary intensifications (PBIs) in the aurora.

■ The temporal evolution of convection properties such as the cross-polar cap potential (CPCP) drop and flow channels at the dawn-dusk polar cap (PC) boundaries around the time of the electrojet events are investigated. Flow channel is defined as a latitudinally restricted (few 100 km) regime of enhanced (> 1 km/s) antisunward convection.

■ Interhemispheric symmetries/asymmetries in the CPCP and in the presence of newly-discovered convection channels at the dawn or dusk side PC boundaries are determined.

■ We distinguish between dayside and nightside sources of PC convection.

Observational Summary: 20 March 2001

■ The interplanetary data are shown in figure 1. Our main focus here will be on the interval 12-17 UT. The panels (from top to bottom) displays, in GSM coordinate: proton number density, temperature, bulk speed, dynamic pressure, total field, the x-, y- and z-components of the field, proton plasma beta, Alfvén Mach number in red in the same panel, IMF clock angle and finally the Boyle potential.

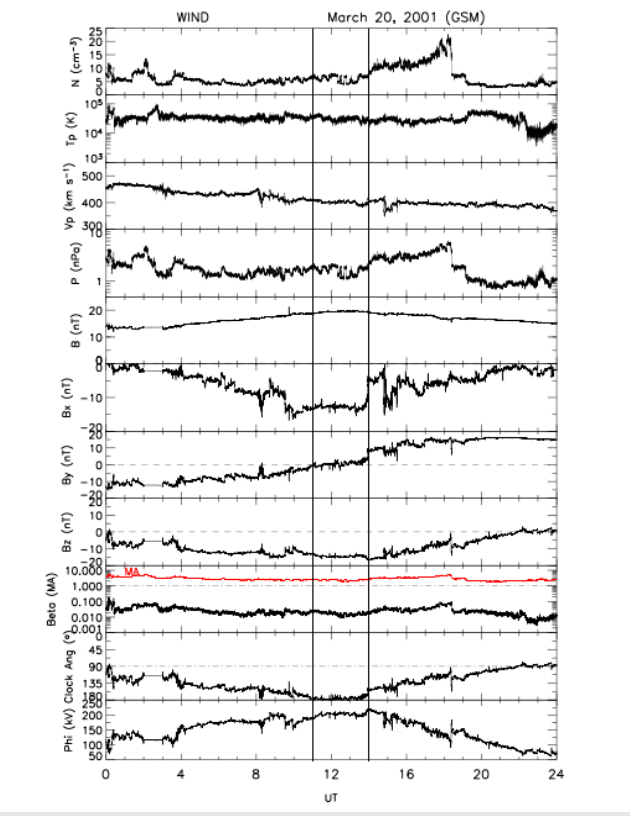


Figure 1: IMF parameters

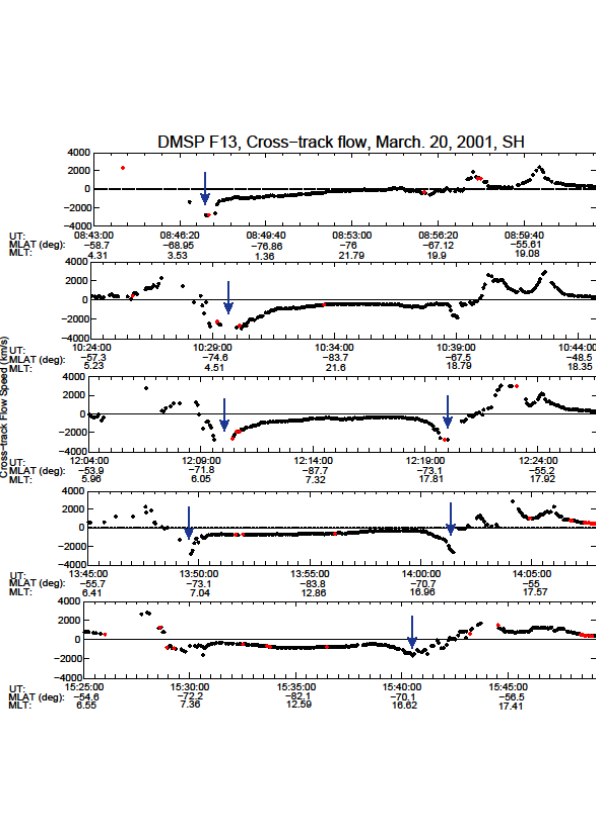


Figure 2: SH cross track flows from DMSP F13

■ This ICME interval shows three consecutive stages characterized by $By < 0$, $By \sim 0$, and $By > 0$ respectively B_z is negative throughout.

■ Characteristics of the ICME-conditions and disturbance levels during four similar cases are listed in table 1.

■ The cross track flows for five DMSP F13 passes in the SH are shown in figure 2. They show clear channels of enhanced antisunward flow (Sandholt et. al., 2009 and Farrugia et. al. 2004) at the polar cap boundary on the dawn/dusk side depending on the IMF By component ($By < 0$, $By = 0$, and $By > 0$).

Date	B_T (nT)	B_z (nT)	B_y (nT)	θ	V (km/s)	n (cm ⁻³)	Dst (nT)	E_{KL} (mV/m)	P_{dyn} (nPa)
20 Mar. 2001	19	-20	0	$\sim 180^\circ$	400	7	-141 (-134/-149)	7.60	1.1-2.1
18 Aug. 2003	17.5	-14	-10	$\sim 150^\circ$	450	2	-136 (-121/-148)	7.35	1-3
20 Nov. 2003	40-60	-20(-50)	40-0	$90^\circ-180^\circ$	600-650	8-30	-102 (-49/-171)	26.68	4-30
30 May 2005	16	-15	-5(-10)	$140^\circ-160^\circ$	450	10	-42(-35/-52)	6.27	5-8

Table 1: Interplanetary and Dst conditions for four intervals of ICME passage at Earth

■ Figure 3-4 shows two consecutive DMSP F13 passes from SH and NH with panels showing particle precipitation, cross-track ion flows and magnetic field perturbations/FACs representing the interval of strongly south ICME magnetic field.

■ The DMSP F13 pass at 1354 UT in the SH shows flow channels on both sides reaching velocities of over 3km/s. The pass in the NH at 1445 UT shows enhanced convection on the dawn side only.

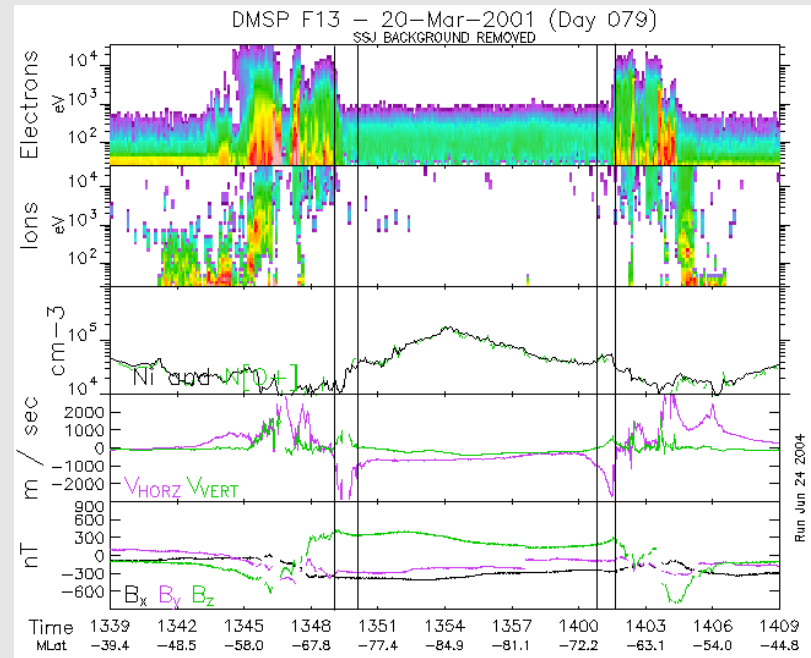


Figure 3: DMSP F13 pass 1339-1409 in the SH.

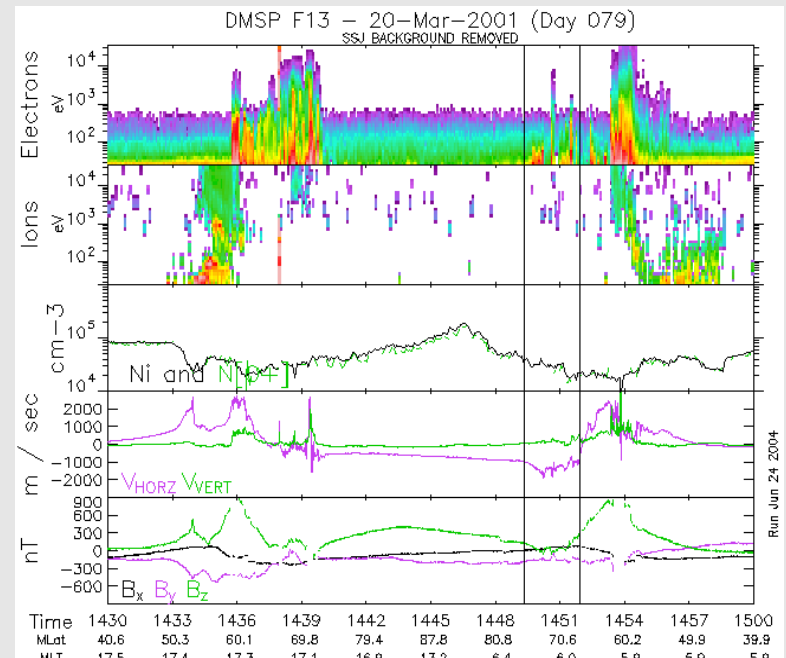


Figure 4: DMSP F13 pass 1430-1500 in the NH.

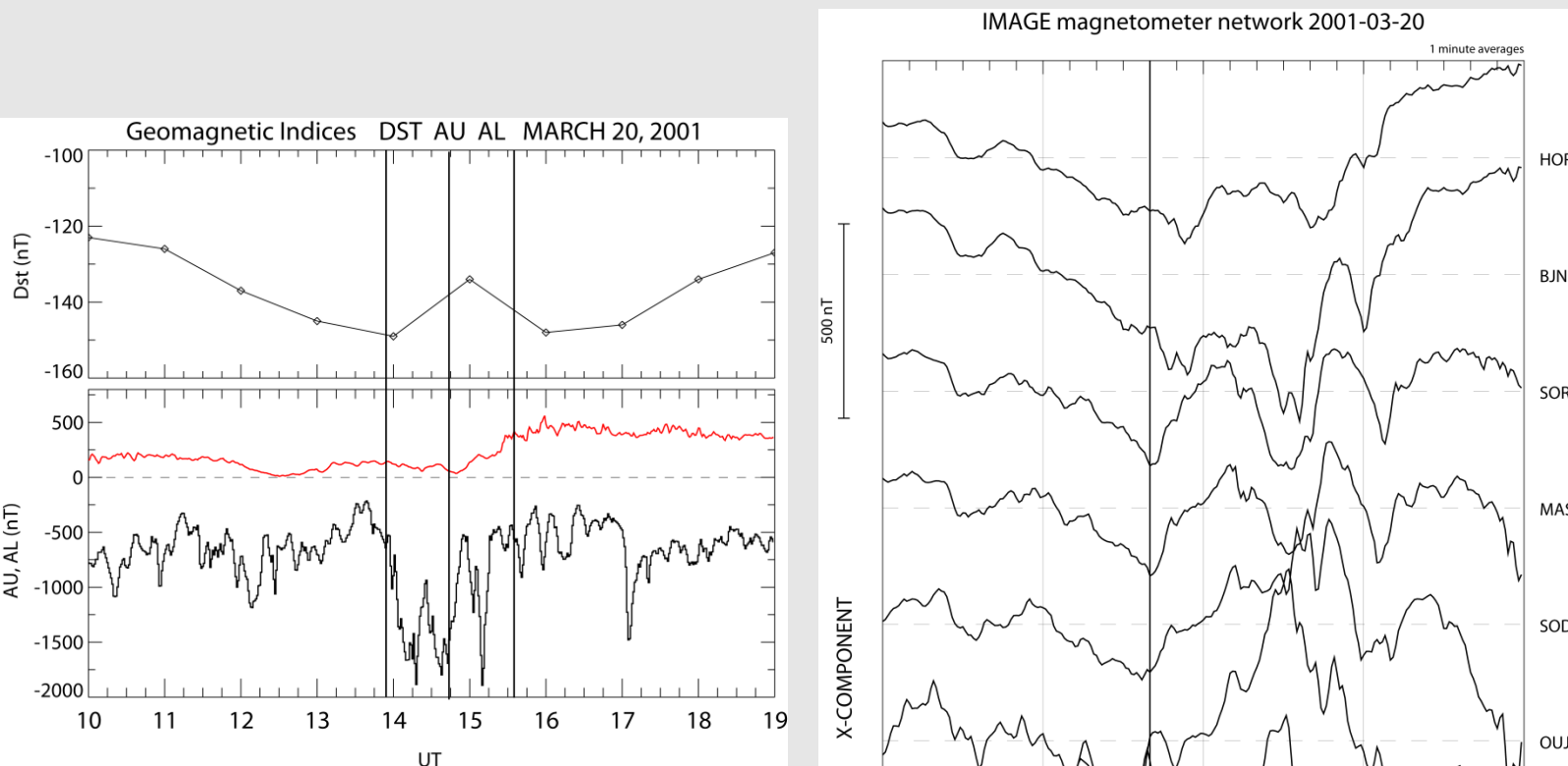


Figure 5: Dst, AU and AL index data. Times of 3 F13 polar cap passes marked by vertical guidelines

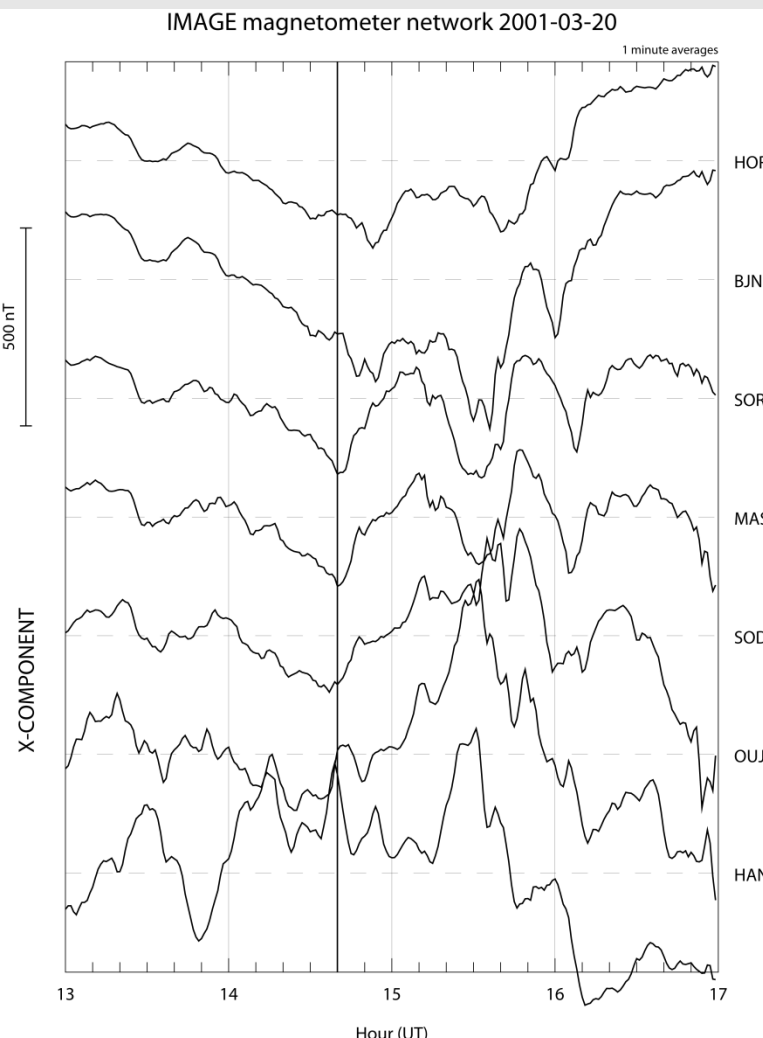


Figure 6: IMAGE magnetometer data for the interval 13-17 UT

■ From the IMAGE magnetometer data (figure 6) we observe a westward electrojet (WEJ) intensification at 1440 UT in the regime of plasma sheet precipitation at $\sim 67^\circ$ MLAT. The eastward electrojet (EEJ) signatures are seen at the HAN (59°) and OAU (61°) stations.

■ The Dst, AU and AL indices (figure 5) show strong activity. We notice three major AL-deflections in the interval 1400-1520UT. The negative deflection in the AL index at 1440 UT coincides with the NH DMSP pass shown in figure 4 and with the electrojet deflection signatures in the IMAGE data.

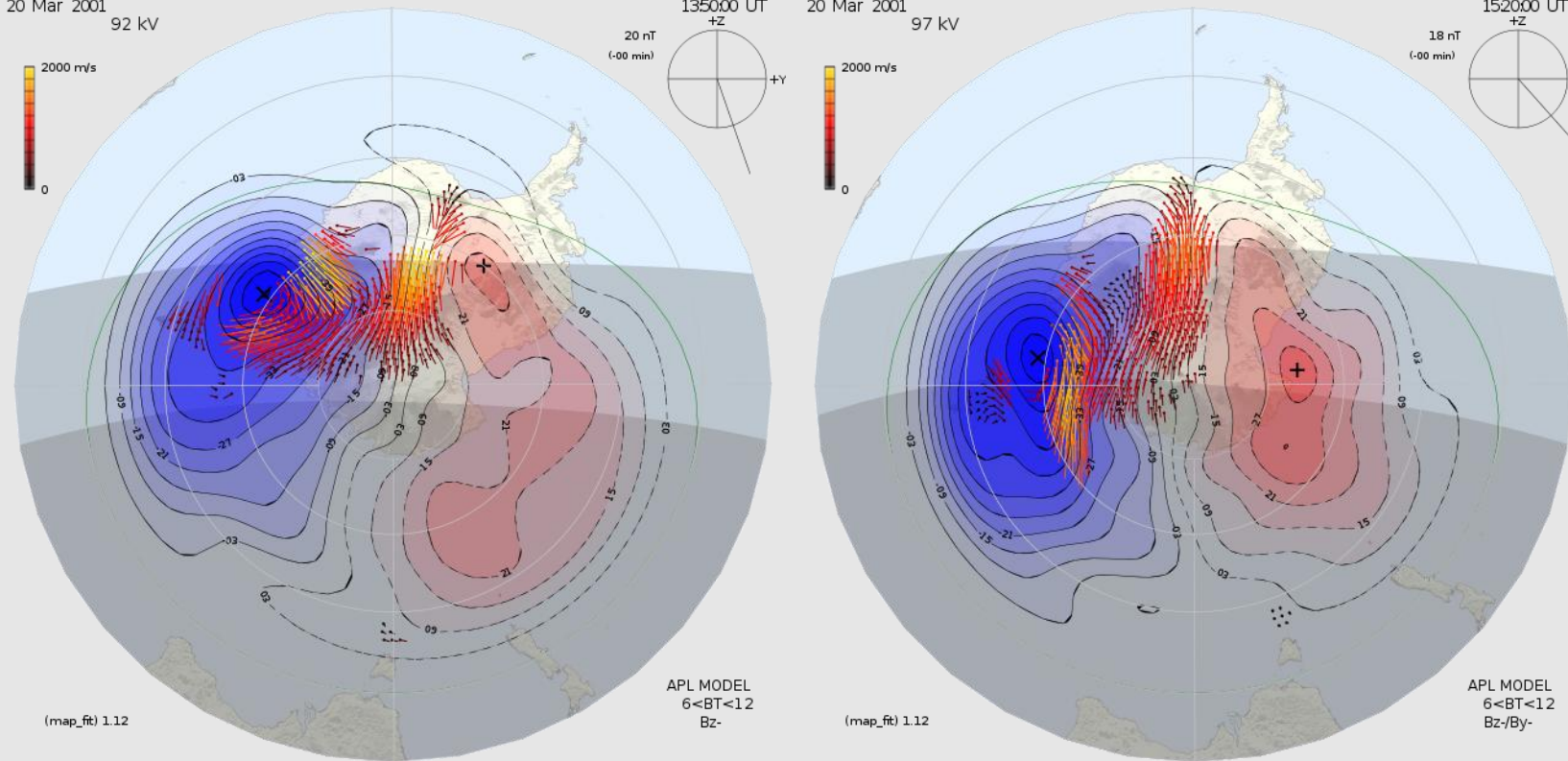


Figure 7: SuperDARN convection plot SH at 1350UT

■ Strong flows are seen in SH with SuperDARN at 1350 (fig. 7) and 1520 UT (fig. 8).

■ The 1350UT radar scan shown in figure 7 is at the same time as the DMSP F13 pass in figure 3. We conclude that flow channels are present on both the dusk and dawn sides in the SH.

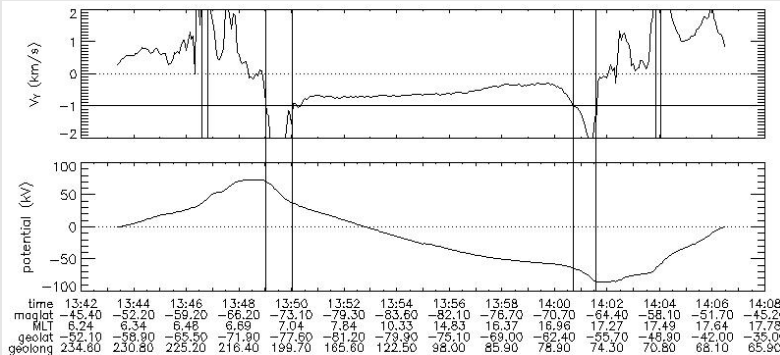


Figure 9: DMSP F13 pass in the SH 1342-1408UT

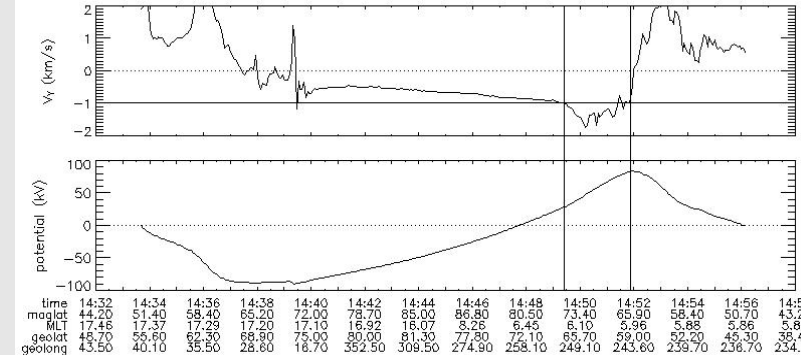


Figure 10: DMSP F13 pass in the NH 1432-1458UT

■ Figures 9 and 10 show the polar cap potential for the SH pass at ~ 1400 and NH pass at ~ 1445 UT. The cross-polar cap potential difference is naturally quite large in both hemispheres as we have very active conditions. The NH pass shows a cross polar cap potential (CPCP) of 174 kV while the SH-pass shows 158 kV.

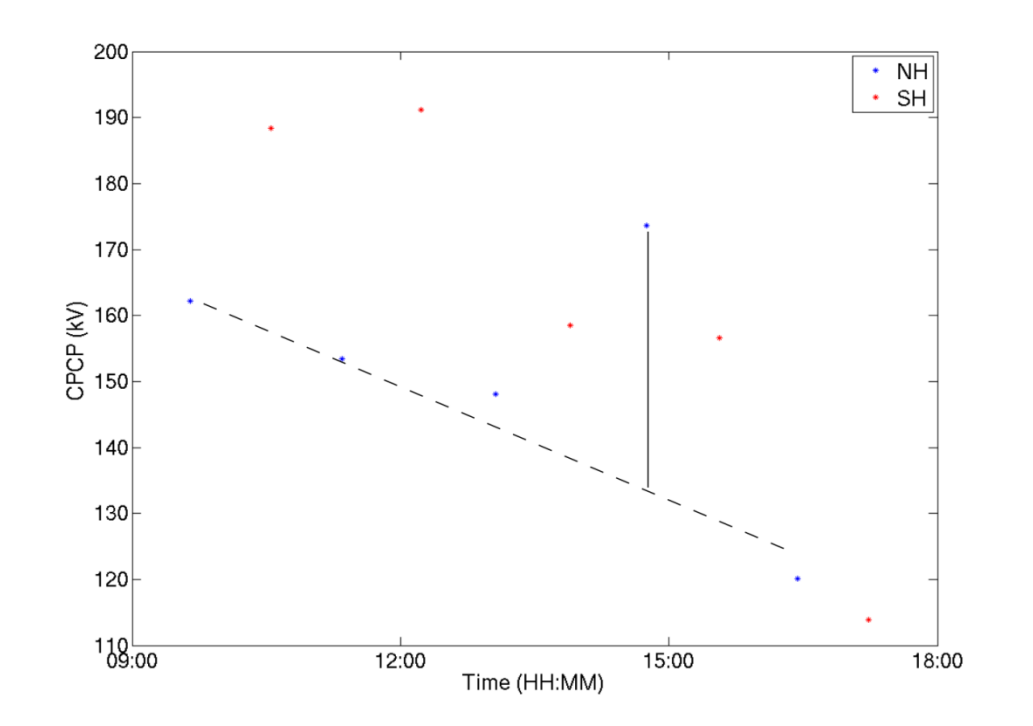


Figure 11: CPCP for the NH (blue) and the SH (red)

■ This is the only interval (1440-1450) where the CPCP is greater in the NH. Table 2 shows the CPCP for all DMSP F13 passes in both hemispheres between approximately 9 UT and 1730 UT where the time given in the table corresponds to the middle of the pass. We see that in general the CPCP is greater in the SH with the exception of the 14:45 UT pass.

■ Figure 11 shows a plot of the CPCP for the northern (blue line) and southern (red line) hemisphere. We see that the blue peaks above the red at 1445 UT.

■ Figure 12 show sketches of the observation-geometry with DMSP F13 s/c crossings in the NH on top and SH below. The electrojets are indicated in the NH, as well as the most relevant magnetometer stations. Arrows marks the flow channels with the potential drop over the channel indicated in parenthesis below.

Time (UT)	CPCP NH (kV)	Time (UT)	CPCP SH (kV)
9:39	162.23	10:33	188.35
11:21	153.47	12:14	191.16
13:04	148.08	13:54	158.46
14:45	173.59	15:34	156.64
16:26	120.1	17:14	113.88

Table 2: CPCP in the northern and southern hemisphere inferred from DMSP F13 ion drift data.

■ Figure 13 shows the dusk side of the northern hemisphere. The WEJ and EEJ are indicated as well as the convection and the position and direction of the C1-C2 and R1-R2 Birkeland currents. These currents have been observed from satellites by Papitashvili et. al. (2002). Plasma flow channels on newly open and old open field lines have been marked FC1 and FC2, respectively (Sandholt et. al., 2009 and Farrugia et. Al. 2004). Convection jets in the pre-midnight sector have been reported by Wang et al. (2010).

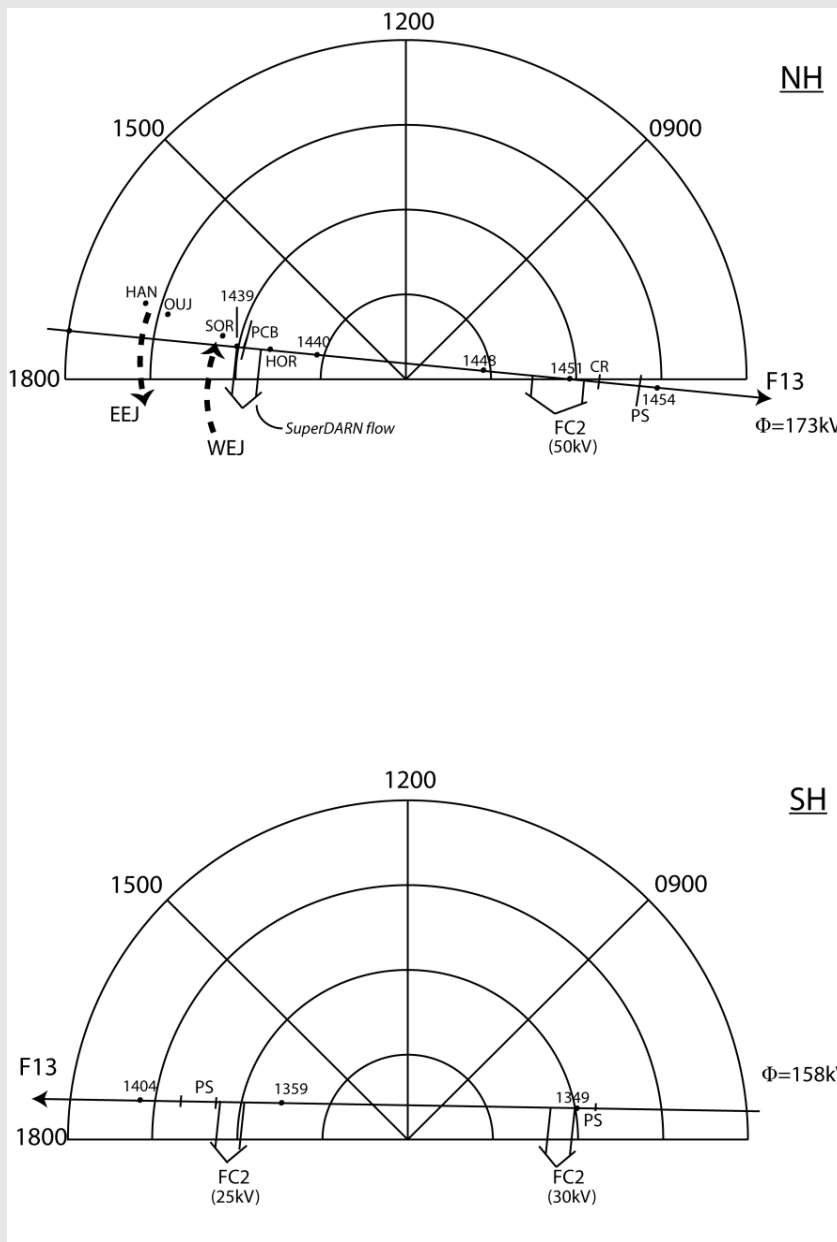


Figure 12: SH and NH DMSP F13 trajectories

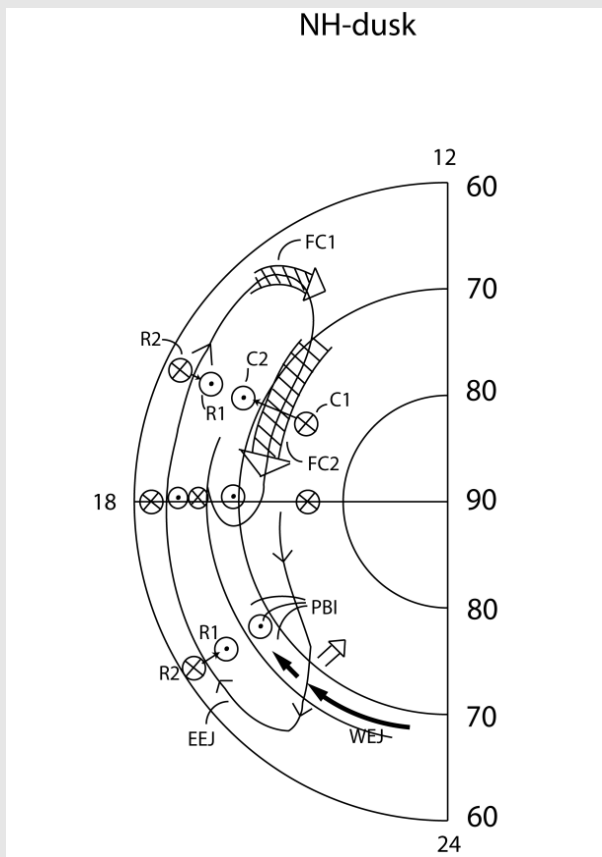


Figure 13: sketch of the NH dusk side indicating the electrojets, flow channels and Birkeland currents.

Conclusions

■ We have here studied polar cap convection during the ICME passage on 20 March 2001 using DMSP satellites, SuperDARN radars and magnetometer data.

■ A dawn-dusk asymmetry depending on the clock angle (By polarity) is present with the three stages $By < 0$, $By \sim 0$, and $By > 0$ giving channels of enhanced antisunward flow on dusk, dusk+dawn and dawn side respectively, for the northern hemisphere and oppositely in the SH.

■ The CPCP inferred from F13 ion drift data also show a clear north-south asymmetry, possibly due to interhemispheric conductivity differences.

■ The AL-index is used as indicator of electrojet/substorm activity. In this case enhanced AL-deflections are observed during the interval 1400-1510 UT.

■ A significant increase (to 173 kV) in CPCP-NH is observed in the interval 1440 - 1450 UT, after major WEJ events ($AL = -1700$ nT) in the interval 1400 - 1450 UT. This enhancement (~ 30 kV) is attributed to an active magnetotail source of polar cap convection (see also Provan et al., 2004, Lockwood et al., 2009, and Kullen et al., 2010).

■ At this time (1450 UT) the dawn - side flow channel, appearing after the two strong electrojet events (1400-1440 UT), contributed approximately 50 kV of the enhanced CPCP-NH (fig. 10).

■ The CPCP-SH observed before (1350 - 1400 UT) and after (1520 - 1540 UT) the WEJ events (approximately 155 kV) is attributed to the magnetopause source (see the SuperDARN convection plots in Figs. 7 and 8).

■ This interpretation is supported by the SuperDARN SH convection pattern at 1350 UT (fig. 7) which looks like a pattern caused by unbalanced dayside reconnection (see Cowley and Lockwood, 1992).

References

■ Cowley, S. W. H. and Lockwood, M., Excitation and decay of solar wind-driven flows in the magnetosphere-ionosphere system, Ann. Geophys., 10, 103-115, 1992.

■ Farrugia, C. J. et. Al. Pulsed flows at the high-altitude cusp poleward boundary, and associated ionospheric convection and particle signatures, during a CLUSTER - FAST - SuperDARN - Sondrestrom conjunction under a southwest IMF, Ann. Geophys., 22, 2891-2905, 2004.

■ Kullen, A., T. Karlsson, J. A. Cumnock, and T. Sundberg., Occurrence and properties of substorms associated with pseudobreakups, J. Geophys. Res., 115, A12310, doi:10.1029/2010JA015866, 2010.

■ Lockwood, M., M. Hairston, I. Finch, and A. Roillard, Transpolar voltage and polar cap flux during the substorm cycle J. Geophys. Res., 114,A0120,doi:10.1029/2008JA013697, 2009.

■ Papitashvili V. O., F. Christiansen, and T. Neubert., A new model of field-aligned currents derived from high-precision satellite magnetic field data, Geophys. Res. Lett., 29, 14, doi:10.1029/2001GL014207, 2002.

■ Provan G., M. Lester, S. B. Mende, and S. E. Milan., Statistical study of high-latitude plasma flow during magnetospheric substorms, Ann. Geophys., 22, 3607-3624, 2004.

■ Sandholt P. E. and C. J. Farrugia. Plasma flow channels at the dawn/dusk polar cap boundaries: momentum transfer on old open field lines and the roles of IMF B_y and conductivity gradients, Ann. Geophys., 27, 1527-1554, 2009.

■ Wang, H., H. Lühr, and A. J. Ridley. Plasma convection jets near the poleward boundary of the nightside auroral oval and their relation to Pedersen conductivity gradients, Ann. Geophys., 28, 969-976, 2010.

Acknowledgements

Access to the DMSP data base (<https://swx.plh.af.mil>) was kindly provided by Air Force Geophysics Research Laboratory, Hanscom, Mass. Ground magnetograms from the Svalbard IMAGE chain of ground stations were obtained from <http://www.geo.fmi.fi/image>. Thanks to Ari Viljanen and Truls Lynne Hansen for operating the IMAGE chain. SuperDARN convection plots were obtained from <http://superdarn.jhuapl.edu>. Work at University of Oslo is supported by the Norwegian Research Council (NFR). Work at UNH is supported by NASA grants NNX08AD11G. and NNX10AQ29G.